Pel-Adaptive Model-Based Interpolation of Spatially Subsampled Images

by

Babak Ayazifar

B.S., Electrical Engineering
California Institute of Technology
(June 1989)

Submitted to the
Department of Electrical Engineering and Computer Science
in partial fulfillment
of the requirements for the degree of

Master of Science

at the

MASSACHUSETTS INSTITUTE OF TECHNOLOGY

February 1992

Author_____
Department of Electrical Engineering and Computer Science
February 11, 1992

Certified by_____
Jae S. Lim
Professor of Electrical Engineering
Thesis Supervisor

Accepted by_____
Campbell L. Searle
Chairman, Departmental Committee on Graduate Students

Pel-Adaptive Model-Based Interpolation of Spatially Subsampled Images

by

Babak Ayazifar

Submitted to the Department of Electrical Engineering and Computer Science
on February 11, 1992, in partial fulfillment of the
requirements for the degree of
Master of Science

Abstract

In this thesis a scheme is proposed for interpolation of spatially subsampled images. The theoretical formulation is based on the fundamental assumption that luminance remains constant along the generalized "path of motion" of a pixel in the image plane. This *Constant Luminance Model (CLM)* of the intensity function in turn leads to a constraint equation, the solution to which is used to compute the unknown intensities. Due to the generalized nature of the algorithm, the most highly visible artifact associated with previously developed methods is significantly suppressed, thereby resulting in noticeably enhanced reconstructed images.

Thesis Supervisor: Jae S. Lim
Title: Professor of Electrical Engineering

Acknowledgments

Praise and glory are due, first and foremost, to Allah (SWT), the Lord of all there is. Were it not for His beneficence and mercy, I simply would not have been. He is the One from whose grace I have derived all my sustenance and strength, and He it is to whom I pledge my undivided allegiance.

Never did I anticipate how daunting a task it would be to have to express deserving gratitude to all those whose kindness and companionship have so deeply affected and enriched my life. What follows in the few humble lines ahead, therefore, merely reflects a failure on my part to adequately display my appreciation of those who have so strongly contributed to my well-being, and I beg forgiveness, in advance, from all those who have received a less-than-deserving attention.

To begin, I would like to thank my research advisor, Professor Jae S. Lim, who granted me the opportunity to develop and nurture in a truly world-class research group. My experiences in the past two years have been unmatched by any other, and they have contributed significantly to my learning and professional development.

The students in the Advanced Television and Signal Processing (ATSP) group, and the Digital Signal Processing Group (DSPG) here at MIT have strongly influenced my personal and academic life throughout the past two years. Among them, two very good friends deserve special mention. My warmest thanks and deepest appreciations go to Shiufun Cheung who has contributed in a very significant way to the development of this thesis. I can never repay him for all the time and effort he put into our various technical discussions; nor can I begin to thank him for his instrumental role in the preparation of the final version of this manuscript. Julien Nicolas is another good friend who made valuable contributions to the development of the theory for this thesis in the early stages, and also assisted me in many program debugging efforts.

Further thanks go to our administrative assistants, Cindy LeBlanc and Debra Harring, for all their help, and all those birthday cakes and fresh early-morning bagels. I would also like to thank Deborah Gage of the DSPG for her extremely valuable assistance on many occasions.

I also wish to extend my gratitude to two very influential people in the EECS graduate office who at times have helped me immensely: Ms. Marilyn Pierce for her assistance on various departmental policy matters, extensions, etc., and Ms. Peggy Carney for her granting me of a departmental fellowship to keep me going in the Summer of 1991.

Acknowledgments-(Continued)

Finally, there are three very dear people whose acknowledgement I have deliberately postponed to the very last slot, because I have found it beyond my capabilities to express in words my true feelings towards them. They are my parents and my sister. I can not even begin to imagine how a son is to thank two parents who give up a lifetime of their earnings to emigrate to a land two continents away, whose language they do not know, and whose culture they do not fully grasp, so that their children can be assured of a brighter future. I am a son in exactly that situation, and I can only hope that I have been able to deliver even a tiny fraction of what they have invested in me in both emotional and financial terms. Along with my sister, their love, affection, and support have been crucial in my survival, and I am eternally grateful to them for all their kindness.

This research has been sponsored by the Center for Advanced Television Studies (CATS), Cable Laboratories Inc., and the National Science Foundation. Current members of the CATS Consortium are ABC, Ampex, Eastman Kodak, General Instrument, Motorola, NBC, NBC Affiliates, PBS, Tektronix, and Zenith. The views expressed herein are the author's and may not represent those of the research sponsors.

Dedications

Think not of those who are slain in the way of Allah as dead. Nay, they live, finding their sustenance in the presence of their Lord.

Holy Qur'an (3:169)

To the memory of my beloved cousin,

Martyr Mostafa Heydarnia,

who helped rekindle the torch of righteousness with his colorful blood, as it was brutally spilt over the deserts, by the sinister mercenaries of the "Butcher of Baghdad."
And to the memory of all those who rushed in heeding the call of the "Prince of the Martyrs," Hossein ibn Ali (peace be upon them both), and rose against evil and hideous aggression.
May God rest their souls, and grant patience and forbearance to the loved ones they have left behind.

تقدیم:

- به روح مطهر پسرخاله و برادر بسیار عزیزم،

شهید مصطفی حیدرنیا

- و به روان پاك تمامی شهدای راه حق، که ندای سیدالشهدای مسلمین، حسین بن علی(ع)، را لبیك گفته و با سلاح ایمان لایتزلزل خود، همواره به جبهه‌های نبرد حق علیه باطل شتافتند، و عاقبت نیز با خون رنگین خویش مشعل صراط توحید را برافروخته، و در پی این آرمان مقدس، ردای سرخ شهادت بر تن نهادند.

یادشان گرامی و مکتبشان پر رهرو باد.

Contents

List of Figures

Chapter 1

Introduction

The problem of spatial interpolation arises in many applications, among which are interlaced-to-progressive-scan conversion[1], VCR freeze-frame for which better vertical resolution is sought by displaying the entire picture frame instead of just one field, image spatial expansion, and video standards conversion between European and American systems in which vertical resampling must be performed to convert between the 625 $\frac{lines}{frame}$ and the 525 $\frac{lines}{frame}$ scan rates. The approaches to this problem, which have been used in the past, can be classified into two main categories.

The first comprises "blind" methods which consider an image simply as a two-dimensional matrix whose element values are the pixel intensities. Schemes involving pixel replication (*i.e.*, zero-order hold), local averaging (*i.e.*, first-order hold), and polynomial interpolation (including spline) all fall under this category. A comparative study of these methods and a thorough discussion of B-spline image filtering is

[1] One example is the conversion of CCIR 601 interlaced video [1] to and from the progressive scan Source Input Format (SIF) video which must be performed at the pre and postprocessor blocks of current MPEG-based digital transmission system proposals.

presented by Hou and Andrews [2].

The second classification of spatial interpolation methods consists of those which have as their premise some realistic and intuitive model of an image, based on which a scheme is developed for computing the unknown intensities. These methods are by far the most promising in comparison with those of the first category.

The algorithm presented in this thesis is a generalization of previous work by Martinez, Lim, and Isnardi [3, 4] in which they describe a frame reconstruction method based on the *Line Shift Model (LSM)*, an essentially motion-compensated interpolation scheme where the dimensionality of the motion is one less than that of the well-known problem of video-sequence temporal interpolation[2]. In the problem of deinterlacing, for example, Martinez [3, 5] performs vertical interpolation by computing shifts between small neighborhoods of adjacent field lines, based on the *LSM*. Once computed, these displacements are projected onto adjacent field lines, in order to pinpoint the pixels whose intensities correspond to the current pel. It then becomes straightforward to extract the unknown intensity of the pel associated with the computed shifts. Figure (1-1) illustrates this algorithm.

This scheme, for the most part, produces interpolated images of noticeably high quality, as Figure (1-2) depicts. The figure consists of the original picture frame, one of the interlaced fields, and the reconstructed frame obtained by applying the *LSM*–based interpolation algorithm of Martinez. As can be noted, however, along contours which are close in slope to the horizontal, such spatial movement computations lead to

[2]Appendix (A) reviews the 3-dimensional motion-compensated spatio-temporal interpolation algorithm, which is an extension of the 2-dimensional problem, along with its associated mathematical concepts.

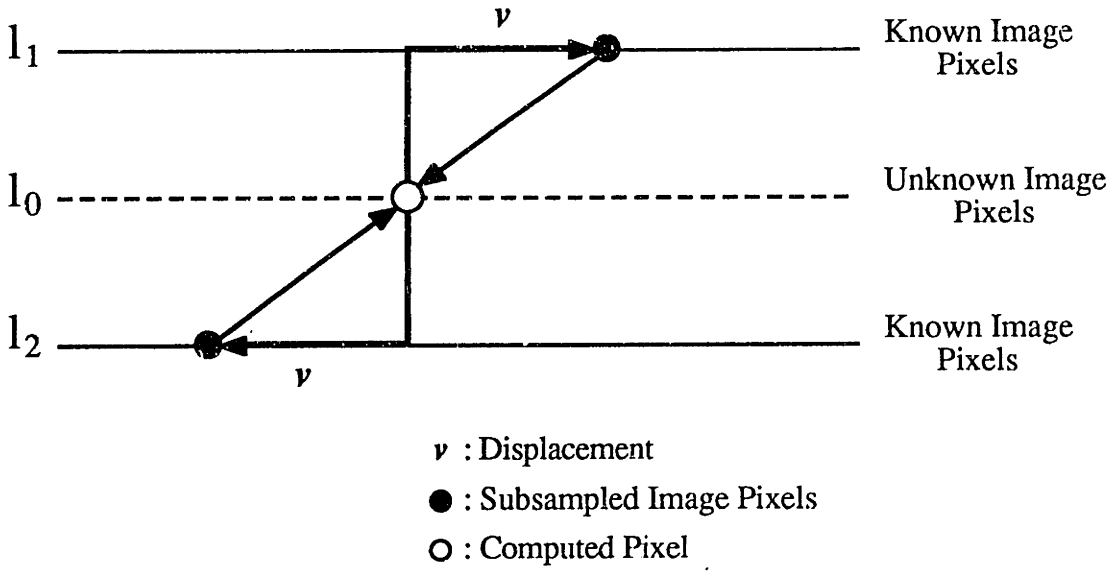

Figure 1-1: Line Shift Model Algorithm

displacement values beyond the dynamic range imposed by the small neighborhood assumption of the *LSM*. Therefore, it becomes necessary to force a zero value on such displacements. This makes the performance of the algorithm in such regions equivalent to that of line averaging, thereby causing all of the artifacts of first-order interpolation, most notably blurring, to manifest themselves along these contours in the processed image.

The proposed algorithm addresses this problem. A model is introduced whereby an image is considered to be composed of concentric circular arcs or "scan curves." Subsequently, the "motion" of a pixel along any contour in the image takes on a parametric nature in which the angular coordinate is radius-dependent (*i.e.*, $I(\varphi(r), r)$ becomes the two-dimensional image model). There are advantages to modeling the pixel motions as radially parametric. In computing the angular displacement, only

those contours which are circles centered at the origin yield the artifacts produced by the previous method. Generally speaking, there are far fewer such curves in typical images than horizontal edges, and, more importantly, a subjective evaluation of numerous pictures has shown that the human visual system is far less sensitive to artifacts in such regions than it is to the prevailing ones along horizontal or vertical directions.

Furthermore, the proposed algorithm improves upon previous results by making not only the origin of the coordinate system but also the method of interpolation pel-adaptive (*i.e.,* Martinez's method is incorporated in the processing scheme in order to handle particular types of contours). By using a simple edge detection scheme, it is determined whether or not an artifact-producing-contour is present at the pixel being processed. If so, the proper interpolation scheme is selected and, based on the orientation of the contour, the coordinate system is changed to one wherein the edge is no longer a curve centered at or near the origin. The corresponding pixel displacement is then solved for, and the proper intensities are used in computing the unknown one. In this manner, even the radial artifacts mentioned earlier are suppressed.

(a)

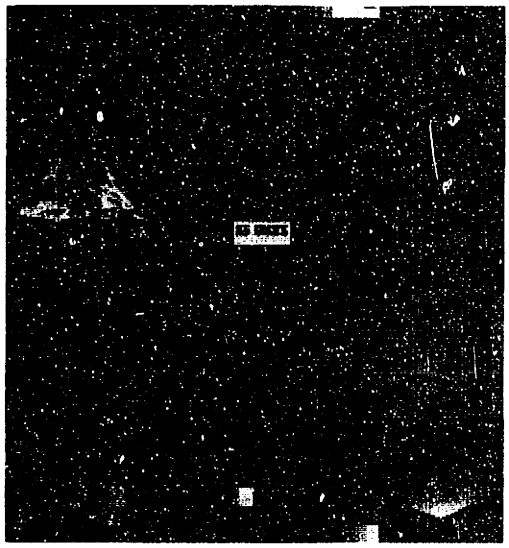

(b)

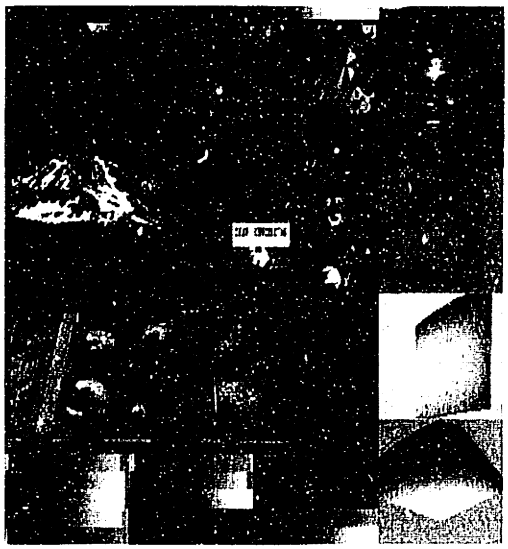

(c)

Figure (1-2):

(a) Original Image
(b) One Field
(c) LSM-Based

Chapter 2

Development of a Generalized Spatial Constraint Equation

2.1 Introduction

We now introduce the fundamental concepts that form the basis of a novel spatial interpolation algorithm. A *Generalized Spatial Constraint Equation (GSCE)* is formulated, using three different methods, each of which casts new intuitive insight over the previous derivations. Underlying the discussion that follows, is a principle generally referred to as the *Constant Luminance Model (CLM)*, which introduces the notion of a parametric "path of motion" for every pixel. The model further asserts that a pel's intensity remains constant as it traverses this path. The path can reside along edges or simply in uniform regions of pictures with varying degrees of uniqueness. In uniform regions, many legitimate paths exist, whereas along edges, the set is restricted to those which run parallel to the discontinuity. A path crossing the edge

contour is unacceptable because it violates the constant luminance assumption.

The goal, therefore, is to estimate the motion (*i.e.*, the displacement which causes the pixel to undergo the least amount of luminance variation), in order to determine the originating and terminating coordinates of the path. The constant luminance assumption may then be invoked and the intensities of the terminal nodes (which ought to be equal) may be assigned to the pixel with the unknown luminance. This process is then iterated for every pel with an unknown intensity.

2.2 Derivation Based on Taylor Expansion

Let $I(\varphi, r)$ denote the intensity of the point (φ, r) on the image plane. The *CLM* then states that this intensity remains constant along the pixel's path of motion as it "moves" to the differentially close neighborhood coordinate $(\varphi + d\varphi, r + dr)$. Hence, we have

$$I(\varphi + d\varphi, r + dr) = I(\varphi, r) \; . \tag{2.1}$$

The desired *Generalized Spatial Constraint Equation (GSCE)* is obtained by expanding the left-hand side of Equation (2.1) by its Taylor series and equating it with the right-hand side, $I(\varphi, r)$. We know, in general, that the Taylor series expansion of a scalar-valued function of a vector-valued argument is given by [6]

$$\psi(\mathbf{t} + \mathbf{a}) = \sum_{n=0}^{\infty} \frac{1}{n!} (\mathbf{a} \cdot \nabla)^n \psi(\mathbf{t}) \tag{2.2}$$

In our case, $\psi(\cdot) = I(\cdot)$ is the image intensity function, $\mathbf{t} = (\varphi, r)$ is the coordinate

vector of the point being processed, $\mathbf{a} = (d\varphi, dr)$ is the differential displacement vector, and $\nabla = (\frac{\partial}{\partial\varphi}, \frac{\partial}{\partial r})$ is the gradient operator. Rewriting Equation (2.2) in terms of the relevant functions and variables yields

$$\begin{aligned} I(\varphi + d\varphi, r + dr) &= I(\varphi, r) + \left(d\varphi \frac{\partial}{\partial\varphi} + dr \frac{\partial}{\partial r} \right) I(\varphi, r) + \\ & \frac{1}{2!} \left(d\varphi \frac{\partial}{\partial\varphi} + dr \frac{\partial}{\partial r} \right)^2 I(\varphi, r) + \cdots \end{aligned} \tag{2.3}$$

where we can reasonably approximate the left-hand side with the first two terms, which are linear, and neglect the effect of all higher order ones. This implies

$$I(\varphi + d\varphi, r + dr) = I(\varphi, r) + d\varphi \frac{\partial I(\varphi, r)}{\partial\varphi} + dr \frac{\partial I(\varphi, r)}{\partial r} \tag{2.4}$$

Comparing Equation (2.1) with Equation (2.4), we note that

$$I(\varphi, r) + d\varphi \frac{\partial I}{\partial\varphi} + dr \frac{\partial I}{\partial r} = I(\varphi, r) \tag{2.5}$$

$$d\varphi \frac{\partial I}{\partial\varphi} + dr \frac{\partial I}{\partial r} = 0 \tag{2.6}$$

$$\frac{d\varphi}{dr} \frac{\partial I}{\partial\varphi} + \frac{\partial I}{\partial r} = 0 \tag{2.7}$$

Defining $v_\varphi = \frac{d\varphi}{dr}$ as the angular shift (*i.e.* units of $^\circ/\hat{\mathbf{r}}$), the desired *Generalized Spatial Constraint Equation (GSCE)* becomes

$$v_\varphi \frac{\partial I}{\partial\varphi} + \frac{\partial I}{\partial r} = 0 \, . \tag{2.8}$$

2.3 Derivation Based on Radial Differentiation

The *GSCE* can be derived from the *CLM* in a much more straightforward manner by recognizing that the radial derivative of $I(\varphi(r), r)$ must be zero as a consequence of the luminance remaining constant over the parametric, radius-dependent path of motion of the pixel being processed. In other words, we must have

$$\frac{d}{dr} I(\varphi(r), r) = 0 \tag{2.9}$$

$$\frac{d\varphi}{dr}\frac{\partial I}{\partial \varphi} + \frac{\partial I}{\partial r} = 0 \tag{2.10}$$

$$v_\varphi \frac{\partial I}{\partial \varphi} + \frac{\partial I}{\partial r} = 0\,, \tag{2.11}$$

where Equation (2.11) is identical to the *GSCE* (2.8) which was obtained in Section (2.2) .

2.4 Derivation Based on the Concentric Circular Shift Model (CCSM)

The *GSCE* may be formulated more intuitively, as was the *Line Shift Model (LSM)* of Isnardi and Martinez [3, 4]. Consider a region of the image in the vicinity of the point (φ_0, r_0), whose luminance is to be computed. Given that the chosen neighborhood is sufficiently small, it would be reasonable to consider adjacent concentric arcs of the image to be related simply by an angular shift v_φ, as denoted by the circular "scan lines" r_1 and r_2 in Figure (2-1). This, with the *Constant Luminance Model (CLM)*,

imply that the intensities of the points on two adjacent arcs, corresponding to the terminal nodes of the path of motion, are equated as follows

$$I(\varphi(r), r) = I(\varphi - \Delta\varphi, r_0) = I_0(\varphi - \Delta\varphi) \ , \tag{2.12}$$

where $\Delta\varphi = v_\varphi(r - r_0)$. Hence we have

$$I(\varphi(r), r) = I_0(\widehat{\varphi}(r)) \ , \tag{2.13}$$

where

$$\widehat{\varphi}(r) = \varphi - \Delta\varphi = \varphi - v_\varphi(r - r_0) \tag{2.14}$$

By taking the partial derivative of the intensity $I(\varphi(r), r)$ with respect to each of the variables, we obtain

$$\begin{aligned} \frac{\partial I}{\partial \varphi} &= \frac{\partial I_0}{\partial \widehat{\varphi}} \frac{\partial \widehat{\varphi}}{\partial \varphi} \\ &= \frac{\partial I_0}{\partial \widehat{\varphi}} \end{aligned} \tag{2.15}$$

and similarly,

$$\begin{aligned} \frac{\partial I}{\partial r} &= \frac{\partial I_0}{\partial \widehat{\varphi}} \frac{\partial \widehat{\varphi}}{\partial r} \\ &= \frac{\partial I}{\partial \varphi} \frac{\partial \widehat{\varphi}}{\partial r} \ . \end{aligned} \tag{2.16}$$

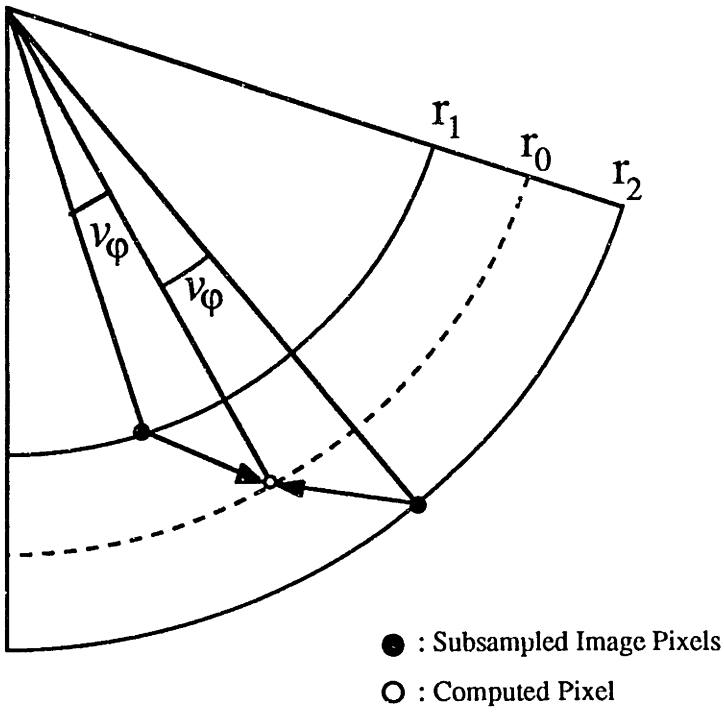

Figure 2-1: Concentric Circular Shift Model

Referring to Equation (2.14), we can rewrite Equation (2.16) as follows

$$\frac{\partial I}{\partial r} = \frac{\partial I}{\partial \varphi}(-v_\varphi) \quad , \tag{2.17}$$

which by rearranging the terms yields

$$v_\varphi \frac{\partial I}{\partial \varphi} + \frac{\partial I}{\partial r} = 0 \quad . \tag{2.18}$$

This is identical to the GSCE (2.8) obtained in Section (2.2) .

2.5 Proof of Generality

We now illustrate how the *GSCE* is a generalization of Martinez's [3, 5] spatial constraint equation. Letting $r = y$, we know that $dr = dy$ and

$$I(\varphi(r), r) = I(\varphi(y), y) \tag{2.19}$$

Therefore, the radial derivative is given by

$$\begin{aligned} \frac{d}{dr} I(\varphi(r), r) &= \frac{d}{dy} I(\varphi(y), y) && (2.20) \\ &= \frac{d\varphi}{dy}\frac{\partial I}{\partial \varphi} + \frac{\partial I}{\partial y} && (2.21) \\ &= 0 \quad . && (2.22) \end{aligned}$$

Lemma 1 *For an image intensity function, I, the following relation holds:*

$$\frac{d\varphi}{dy}\frac{\partial I}{\partial \varphi} = \frac{dx}{dy}\frac{\partial I}{\partial x}. \tag{2.23}$$

Proof:

$$\begin{aligned} \frac{d}{dy} I(x(y), y) &= \frac{\partial I}{\partial x}\frac{dx}{dy} + \frac{\partial I}{\partial y} && (2.24) \\ \frac{\partial I}{\partial x}\frac{dx}{dy} &= \frac{d}{dy} I(x(y), y) - \frac{\partial I}{\partial y} && (2.25) \\ \frac{d}{dy} I(\varphi(y), y) &= \frac{\partial I}{\partial \varphi}\frac{d\varphi}{dy} + \frac{\partial I}{\partial y} && (2.26) \\ \frac{\partial I}{\partial \varphi}\frac{d\varphi}{dy} &= \frac{d}{dy} I(\varphi(y), y) - \frac{\partial I}{\partial y} \quad . && (2.27) \end{aligned}$$

However, since $I(x(y),y)$ and $I(\varphi(y),y)$ are simply different representations of the same function, we know that

$$\frac{d}{dy}I(x(y),y) = \frac{d}{dy}I(\varphi(y),y) \quad . \tag{2.28}$$

Therefore, we have

$$\frac{dx}{dy}\frac{\partial I}{\partial x} = \frac{d\varphi}{dy}\frac{\partial I}{\partial \varphi} \quad , \tag{2.29}$$

and this completes our proof.

Applying the result of Lemma (1) to Equation (2.22) yields

$$\frac{dx}{dy}\frac{\partial I}{\partial x} + \frac{\partial I}{\partial y} = 0 \quad . \tag{2.30}$$

Defining $v = \frac{dx}{dy}$ we have

$$v\frac{\partial I}{\partial x} + \frac{\partial I}{\partial y} = 0 \quad , \tag{2.31}$$

which is Martinez's spatial constraint equation for vertical interpolation. A similar argument holds for horizontal interpolation, which corresponds to the case where $r = x$.

2.6 Summary

In this chapter three different methods of deriving the *Generalized Spatial Constraint Equation (GSCE)*

$$v_\varphi\frac{\partial I}{\partial \varphi} + \frac{\partial I}{\partial r} = 0 \quad , \tag{2.32}$$

which governs the pixel displacement, v_φ, have been presented. Although the derivations have ranged from mathematical to intuitive, all have been premised on the fundamental concept underlying motion-compensated interpolation schemes, the *Constant Luminance Model (CLM)*. In Chapter 3 it will be shown how the *GSCE* may be solved in order to obtain an estimate for the displacement, v_φ, corresponding to each unknown pixel intensity.

Chapter 3

Solution of the Generalized Spatial Constraint Equation

3.1 Introduction

Now that a *GSCE* has been formulated, we focus our attention on the problem of computing the desired displacement, v_φ. We know from the *Concentric Circular Shift Model (CCSM)* that the solution of the *GSCE* can be thought of as the angular shift between "adjacent" circular arcs surrounding the pixel being processed. By applying the *GSCE* on a local neighborhood basis, we can find the least-squares estimate of v_φ which can, in turn, be projected onto the adjacent arcs in order to find the points to whose intensities the current pixel luminance corresponds. Furthermore, we will note that in estimating v_φ it is necessary to compute the image gradient values at the local neighborhood points. This is done by using a parametric polynomial expansion method where the image is locally modeled as a linear combination of a set of basis

functions. The vector of the local image model parameters (*i.e.*, the coefficients which multiply each of the basis functions to determine the overall linear combination) are determined on a pel-adaptive basis so that the model is updated according to local image characteristics.

3.2 Computation of the Angular Displacement

Normally it is impossible to find a displacement, v_φ, such that the *GSCE* is satisfied at all points within a two-dimensional neighborhood of the pel being processed. This is due to the fact that the *GSCE* must be solved in terms of the displacement, v_φ, at N points in the vicinity of the unknown pixel. That is, we must have

$$\begin{aligned} \left(\frac{\partial I}{\partial \varphi}\bigg|_{P_1}\right) v_\varphi \;+\; \left(\frac{\partial I}{\partial r}\bigg|_{P_1}\right) &= 0 \\ \vdots \qquad\qquad\qquad & \quad , \\ \left(\frac{\partial I}{\partial \varphi}\bigg|_{P_N}\right) v_\varphi \;+\; \left(\frac{\partial I}{\partial r}\bigg|_{P_N}\right) &= 0 \end{aligned} \tag{3.1}$$

where the P_i's make up the N points of the local neighborhood over which the *GSCE* is applied. This set of N equations in one unknown can be rewritten in vector form as

$$\mathbf{I}_\varphi v_\varphi + \mathbf{I}_r = \mathbf{0} \quad , \tag{3.2}$$

or equivalently as

$$\mathbf{I}_\varphi v_\varphi = -\mathbf{I}_r \ , \tag{3.3}$$

where $\mathbf{I}_\varphi$ and $\mathbf{I}_r$ are the angular and radial partial derivatives, respectively, of the intensity vector

$$\mathbf{I} = \begin{bmatrix} I|_{P_1} \\ \vdots \\ I|_{P_N} \end{bmatrix}_{N\times 1} , \tag{3.4}$$

and are given by

$$\mathbf{I}_\varphi = \begin{bmatrix} \left.\frac{\partial I}{\partial \varphi}\right|_{P_1} \\ \vdots \\ \left.\frac{\partial I}{\partial \varphi}\right|_{P_N} \end{bmatrix}_{N\times 1} , \tag{3.5}$$

and

$$\mathbf{I}_r = \begin{bmatrix} \left.\frac{\partial I}{\partial r}\right|_{P_1} \\ \vdots \\ \left.\frac{\partial I}{\partial r}\right|_{P_N} \end{bmatrix}_{N\times 1} . \tag{3.6}$$

To solve for the angular displacement, v_φ, we can multiply both sides of Equation (3.3) by $\mathbf{I}_\varphi{}^T$ to obtain

$$\mathbf{I}_\varphi{}^T \mathbf{I}_\varphi v_\varphi = -\mathbf{I}_\varphi{}^T \mathbf{I}_r , \tag{3.7}$$

which is equivalent to

$$\|\mathbf{I}_\varphi\|^2 v_\varphi = -\mathbf{I}_\varphi{}^T \mathbf{I}_r . \tag{3.8}$$

Furthermore, knowing that $\mathbf{I}_\varphi{}^T\mathbf{I}_\varphi = \|\mathbf{I}_\varphi\|^2$ is a scalar, we simply divide both sides of Equation (3.8) by $\|\mathbf{I}_\varphi\|^2$ to obtain the displacement, v_φ, as follows:

$$v_\varphi = -\frac{\mathbf{I}_\varphi{}^T\,\mathbf{I}_r}{\|\mathbf{I}_\varphi\|^2} \quad . \tag{3.9}$$

It is important to note that the displacement, v_φ, of Equation (3.9) denotes *not* an exact solution of the over-constrained system of equations (3.1), but rather a least-squares solution of it. This can be shown by introducing a constraint residual [3, 5] vector, $\mathcal{E} = [\epsilon_1, \ldots, \epsilon_N]^T$, in Equation (3.2) as follows:

$$\mathbf{I}_\varphi v_\varphi + \mathbf{I}_r = \mathcal{E} \quad . \tag{3.10}$$

In order to find the displacement, v_φ, for a particular spatial position, we assume that the required image gradients at a set of N points in the neighborhood of that coordinate are known[1]. We can then find the displacement corresponding to the pel being processed, by using a least-squares estimator to solve the following minimization problem:

$$\min_{(v_\varphi)}\left\{\|\mathcal{E}\|^2\right\} \equiv \min_{(v_\varphi)}\left\{(\mathbf{I}_\varphi v_\varphi + \mathbf{I}_r)^T(\mathbf{I}_\varphi v_\varphi + \mathbf{I}_r)\right\} \tag{3.11}$$

$$\equiv \min_{(v_\varphi)}\left\{\sum_{i=1}^{N}\epsilon_i{}^2\right\} \quad , \tag{3.12}$$

[1]Section (3.3) deals with the problem of computing the local image gradients.

where

$$\epsilon_i = v_\varphi \left.\frac{\partial I}{\partial \varphi}\right|_{P_i} + \left.\frac{\partial I}{\partial r}\right|_{P_i} \quad , \qquad i = 1, \ldots, N \ . \tag{3.13}$$

denotes the residual at the i^{th} point, P_i , of the neighborhood. Hence, the equivalent minimization problem, which is to be solved, is given by

$$\min_{(v_\varphi)} \left\{ \sum_{i=1}^{N} \left(v_\varphi \left.\frac{\partial I}{\partial \varphi}\right|_{P_i} + \left.\frac{\partial I}{\partial r}\right|_{P_i} \right)^2 \right\} \quad . \tag{3.14}$$

Since the minimization problem depicted by (3.14) involves a quadratic in v_φ, the solution can be obtained by solving a linear equation.

Differentiating the expression, $\|\mathcal{E}\|^2 = \sum_{i=1}^{N} \epsilon_i^2$, with respect to v_φ yields

$$\begin{aligned} \frac{d}{dv_\varphi}\left\{\|\mathcal{E}\|^2\right\} &= \frac{d}{dv_\varphi}\left\{ \sum_{i=1}^{N} \left(v_\varphi \left.\frac{\partial I}{\partial \varphi}\right|_{P_i} + \left.\frac{\partial I}{\partial r}\right|_{P_i} \right)^2 \right\} \\ &= 2\sum_{i=1}^{N} \left[\left(v_\varphi \left.\frac{\partial I}{\partial \varphi}\right|_{P_i} + \left.\frac{\partial I}{\partial r}\right|_{P_i} \right) \left(\left.\frac{\partial I}{\partial \varphi}\right|_{P_i} \right) \right] \\ &= 2\sum_{i=1}^{N} \left[v_\varphi \left(\left.\frac{\partial I}{\partial \varphi}\right|_{P_i} \right)^2 + \left(\left.\frac{\partial I}{\partial \varphi}\right|_{P_i} \right) \left(\left.\frac{\partial I}{\partial r}\right|_{P_i} \right) \right] \quad . \end{aligned} \tag{3.15}$$

Setting the derivative, $\frac{d}{dv_\varphi}\left\{\|\mathcal{E}\|^2\right\}$, equal to zero we have

$$\left[\sum_{i=1}^{N} \left(\left.\frac{\partial I}{\partial \varphi}\right|_{P_i} \right)^2 \right] v_\varphi + \sum_{i=1}^{N} \left(\left.\frac{\partial I}{\partial \varphi}\right|_{P_i} \right) \left(\left.\frac{\partial I}{\partial r}\right|_{P_i} \right) = 0 \quad , \tag{3.16}$$

which leads to the solution

$$v_\varphi = \frac{-\sum_{i=1}^{N} \left(\left.\frac{\partial I}{\partial \varphi}\right|_{P_i} \right) \left(\left.\frac{\partial I}{\partial r}\right|_{P_i} \right)}{\sum_{i=1}^{N} \left(\left.\frac{\partial I}{\partial \varphi}\right|_{P_i} \right)^2} \quad . \tag{3.17}$$

Comparing Equation (3.9) with (3.17) we note that the two forms in which the angular displacement, v_φ, has been written are identical, since we know

$$\mathbf{I}_\varphi{}^T \mathbf{I}_r = \left[\left.\frac{\partial I}{\partial \varphi}\right|_{P_1} \quad \cdots \quad \left.\frac{\partial I}{\partial \varphi}\right|_{P_N} \right] \begin{bmatrix} \left.\frac{\partial I}{\partial r}\right|_{P_1} \\ \vdots \\ \left.\frac{\partial I}{\partial r}\right|_{P_N} \end{bmatrix} \tag{3.18}$$

$$= \sum_{i=1}^{N} \left(\left.\frac{\partial I}{\partial \varphi}\right|_{P_i} \right) \left(\left.\frac{\partial I}{\partial r}\right|_{P_i} \right) \tag{3.19}$$

and

$$\|\mathbf{I}_\varphi\|^2 = \sum_{i=1}^{N} \left(\left.\frac{\partial I}{\partial \varphi}\right|_{P_i} \right)^2 \quad . \tag{3.20}$$

3.3 Computation of the Luminance Gradients

In order to compute the displacement, v_φ, using Equation (3.9), we need to evaluate the vectors $\mathbf{I}_\varphi$ and $\mathbf{I}_r$ at the neighborhood points P_i, $1 \leq i \leq N$. This requires evaluation of the intensity gradients at those neighborhood points. To this end, we follow a procedure analogous to Martinez's.

3.3.1 Parametric Image Model Approximation

We propose a parametric model for the local image intensity function whereby the luminance space is considered to be spanned by a set of P basis functions, as depicted by the following equation:

$$\hat{I}(\varphi, r) = \sum_{j=1}^{P} f_j \psi_j(\varphi, r) \quad . \tag{3.21}$$

Rewriting Equation (3.21) in vector form, we have

$$\hat{I}(\varphi, r) = \Psi^T \mathbf{F} \quad , \tag{3.22}$$

where

$$\Psi = \begin{bmatrix} \psi_1(\varphi, r) \\ \vdots \\ \psi_P(\varphi, r) \end{bmatrix}_{P \times 1} \quad , \tag{3.23}$$

and

$$\mathbf{F} = \begin{bmatrix} f_1 \\ \vdots \\ f_P \end{bmatrix}_{P \times 1} \tag{3.24}$$

denote the basis function vector and the luminance model parameter vector, respectively. The basis function vector comprises a set of P basis functions, which in our

simulations were the following (note that $P = 5$):

$$\begin{aligned} &\psi_1(\varphi, r) = 1 \qquad \psi_2(\varphi, r) = \varphi \qquad \psi_3(\varphi, r) = r \\ &\psi_4(\varphi, r) = \varphi^2 \quad \psi_5(\varphi, r) = r\,\varphi \end{aligned} \quad . \tag{3.25}$$

Moreover, the luminance model parameter vector, $\mathbf{F}$, consists of P coefficients corresponding to the P basis functions. To find the optimal signal model parameters, f_j, we introduce and minimize a least-squares error criterion as follows:

$$\min_{(f_j)} \left\{ \|\mathcal{E}_0\|^2 \right\} \equiv \min_{(f_j)} \left\{ \sum_{k=1}^{M} \left[I(\varphi_k, r_k) - \widehat{I}(\varphi_k, r_k) \right]^2 \right\} \tag{3.26}$$

$$\equiv \min_{(f_j)} \left\{ \sum_{k=1}^{M} \left[I(\varphi_k, r_k) - \sum_{j=1}^{P} f_j \psi_j(\varphi_k, r_k) \right]^2 \right\} \quad . \tag{3.27}$$

The minimization problem (3.27) involves solving a set of M equations in P unknowns. This can be shown by setting the derivative of the squared error, $\|\mathcal{E}_0\|^2$, equal to zero, as depicted by the following:

$$\frac{d}{df_j} \left\{ \|\mathcal{E}_0\|^2 \right\} = \frac{d}{df_j} \left\{ \sum_{k=1}^{M} \left[I(\varphi_k, r_k) - \widehat{I}(\varphi_k, r_k) \right]^2 \right\} \tag{3.28}$$

$$= \sum_{k=1}^{M} \frac{d}{df_j} \left[I(\varphi_k, r_k) - \sum_{j=1}^{P} f_j \psi_j(\varphi_k, r_k) \right]^2 \tag{3.29}$$

$$= -2 \sum_{k=1}^{M} \psi_j(\varphi_k, r_k) \left[I(\varphi_k, r_k) - \sum_{j=1}^{P} f_j \psi_j(\varphi_k, r_k) \right] \tag{3.30}$$

$$= 0 \quad . \tag{3.31}$$

This implies that we must have

$$I(\varphi_k, r_k) - \sum_{j=1}^{P} f_j \psi_j(\varphi_k, r_k) = 0 \ , \qquad k = 1, \ldots, M \ . \tag{3.32}$$

Equation (3.32) can be rewritten as

$$\begin{aligned} \sum_{j=1}^{P} f_j \psi_j(\varphi_1, r_1) &= I(\varphi_1, r_1) \\ &\vdots \\ \sum_{j=1}^{P} f_j \psi_j(\varphi_M, r_M) &= I(\varphi_M, r_M) \quad . \end{aligned} \tag{3.33}$$

The over-constrained set of M equations in P unknowns depicted by (3.33), in turn, can be rewritten in matrix form as

$$A\mathbf{F} = \mathbf{I} \quad , \tag{3.34}$$

where

$$A = \begin{bmatrix} \psi_1(\varphi_1, r_1) & \ldots & \psi_P(\varphi_1, r_1) \\ \vdots & & \vdots \\ \psi_1(\varphi_M, r_M) & \ldots & \psi_P(\varphi_M, r_M) \end{bmatrix}_{M \times P} \quad , \tag{3.35}$$

and

$$\mathbf{I} = \begin{bmatrix} I(\varphi_1, r_1) \\ \vdots \\ I(\varphi_M, r_M) \end{bmatrix}_{M \times 1} \quad . \tag{3.36}$$

It is known from fundamental principles of linear algebra, that the least squares solution to the inconsistent system (3.34) satisfies

$$A^T A\mathbf{F} = A^T\mathbf{I} \quad . \tag{3.37}$$

Provided that the columns of A are linearly independent, $A^T A$, which is a square $P \times P$ matrix, will be invertible and the least squares solution will be given by

$$\mathbf{F} = \left(A^T A\right)^{-1} A^T\mathbf{I} \quad . \tag{3.38}$$

At this juncture, it is worth noting that the parameters N and M referred to throughout the discussion, are completely independent of one another. The quantity, N, represents the number of points in the neighborhood of the unknown pel, and we have denoted these points by P_i where $i \in \{1, \ldots, N\}$. It is at these points that the image gradient needs to be determined in order to compute the displacement, v_φ. However, in order to compute these image gradients, the intensities at a set of M pixels about every P_i are needed. In our simulations, we used the same number for both M and N, but this need not be the case.

3.3.2 Computation of the Gradient Vectors, $\mathbf{I}_\varphi$ and $\mathbf{I}_r$

Having computed the image model parameter vector, $\mathbf{F}$, we can compute the image gradients at any point by referring to Equation (3.21). The gradients are given by

$$\frac{\partial I}{\partial \varphi} = \sum_{j=1}^{P} f_j \frac{\partial \psi_j}{\partial \varphi} = \Psi_\varphi{}^T \mathbf{F} \quad , \tag{3.39}$$

and

$$\frac{\partial I}{\partial r} = \sum_{j=1}^{P} f_j \frac{\partial \psi_j}{\partial r} = \Psi_r{}^T \mathbf{F} \quad , \tag{3.40}$$

where

$$\Psi_\varphi = \begin{bmatrix} \dfrac{\partial \psi_1}{\partial \varphi} \\ \vdots \\ \dfrac{\partial \psi_P}{\partial \varphi} \end{bmatrix}_{P \times 1} , \tag{3.41}$$

and

$$\Psi_r = \begin{bmatrix} \dfrac{\partial \psi_1}{\partial r} \\ \vdots \\ \dfrac{\partial \psi_P}{\partial r} \end{bmatrix}_{P \times 1} . \tag{3.42}$$

We can now rewrite $\mathbf{I}_\varphi$ and $\mathbf{I}_r$ as follows:

$$\mathbf{I}_\varphi = \mathbf{G}_\varphi \mathbf{F} \tag{3.43}$$

and

$$\mathbf{I}_r = \mathbf{G}_r \mathbf{F} \, , \tag{3.44}$$

where

$$\mathbf{G}_{\varphi} = \begin{bmatrix} \left[\left.\frac{\partial \psi_1}{\partial \varphi}\right|_{P_1} \right. & \cdots & \left. \left. \frac{\partial \psi_P}{\partial \varphi} \right|_{P_1} \right] \\ & \vdots & \\ \left[\left.\frac{\partial \psi_1}{\partial \varphi}\right|_{P_N} \right. & \cdots & \left. \left. \frac{\partial \psi_P}{\partial \varphi} \right|_{P_N} \right] \end{bmatrix}_{N \times P} = \begin{bmatrix} \left. {\Psi_{\varphi}}^T \right|_{P_1} \\ \vdots \\ \left. {\Psi_{\varphi}}^T \right|_{P_N} \end{bmatrix}_{N \times P} \tag{3.45}$$

and

$$\mathbf{G}_{r} = \begin{bmatrix} \left[\left.\frac{\partial \psi_1}{\partial r}\right|_{P_1} \right. & \cdots & \left. \left. \frac{\partial \psi_P}{\partial r} \right|_{P_1} \right] \\ & \vdots & \\ \left[\left.\frac{\partial \psi_1}{\partial r}\right|_{P_N} \right. & \cdots & \left. \left. \frac{\partial \psi_P}{\partial r} \right|_{P_N} \right] \end{bmatrix}_{N \times P} = \begin{bmatrix} \left. {\Psi_{r}}^T \right|_{P_1} \\ \vdots \\ \left. {\Psi_{r}}^T \right|_{P_N} \end{bmatrix}_{N \times P} \tag{3.46}$$

are the basis function gradient matrices.

With the image model parameter vector computed, Equations (3.9), (3.43) and (3.44) yield the following estimate for the angular displacement:

$$v_{\varphi} = -\frac{\mathbf{F}^T \, {\mathbf{G}_{\varphi}}^T \, \mathbf{G}_{r} \, \mathbf{F}}{\|\mathbf{G}_{\varphi} \, \mathbf{F}\|^2} \, . \tag{3.47}$$

3.4 Summary

In this chapter, the mathematical development of a solution for the *Generalized Spatial Constraint Equation (GSCE)* has been outlined, and it has been shown that the proposed spatial interpolation algorithm is highly efficient in that the displacement, v_{φ}, computations involve only simple vector/matrix operations. Furthermore, the solution obtained is optimal in the least squares sense, since that is how the underlying error minimization criteria have been defined.

Chapter 4

Development of a Contour-Adaptive Interpolation Algorithm

4.1 Introduction

In this chapter we address the implementational issues of the novel spatial interpolation algorithm, the theory for which was established in Chapters 2 and 3. Recall that we proved the *Generalized Spatial Constraint Equation (GSCE)* to be an extension of Martinez's spatial constraint equation [3, 5]. This property is utilized in constructing a cotour-adaptive algorithm which is capable of resolving a more general class of edge orientations than is the *Line Shift Model (LSM)*-based method proposed by Martinez [3, 5].

4.2 Improvements Due to Increased Adaptivity

The proposed algorithm utilizes both the *Concentric Circular Shift Model (CCSM)* and the *Line Shift Model (LSM)* in computing the unknown intensities. When a pixel is attempted for processing, its local neighborhood is examined for the orientation of the edge on which it resides. An "edge factor," δ, is introduced which contains this orientation information. This edge analysis is performed by selecting three different sets of "adjacent arcs" around the pel being processed, as shown in Figure (4-1). The "edge factor" is then defined as

$$\delta = \sum_{i=1}^{L} \left| \Gamma_i - \Gamma_{(i+\frac{L}{2})} \right| , \tag{4.1}$$

where L, an even number, represents the number of points used in the orientation analysis, and Γ_i denotes the intensity of the i^{th} point.

Notice that the three sets of arc pairs in Figure (4-1) will yield the smallest "edge factor" for those contours to which they are perpendicular or nearly so. The *CCSM* is utilized with the proper origin (*i.e.*, at one of the top corners of the image) if the minimum δ corresponds to the curved arcs which are centered at one of the top image corners. Otherwise, Martinez's scheme is implemented. The algorithm selects the method (*i.e.*, *CCSM* or *LSM*) and the coordinate origin (*i.e.*, top-left or top-right) so as to give preference to edges which are relatively perpendicular to the arc pairs, thereby minimizing the possibility of edge artifacts.

Figure (4-2) shows a high-level system diagram of the adaptive *CCSM*-based spatial interpolator, and Figure (4-3) shows the improvements due to the contour-adaptive algorithm, where the edge artifacts present in Martinez's *LSM*-only method are significantly suppressed.

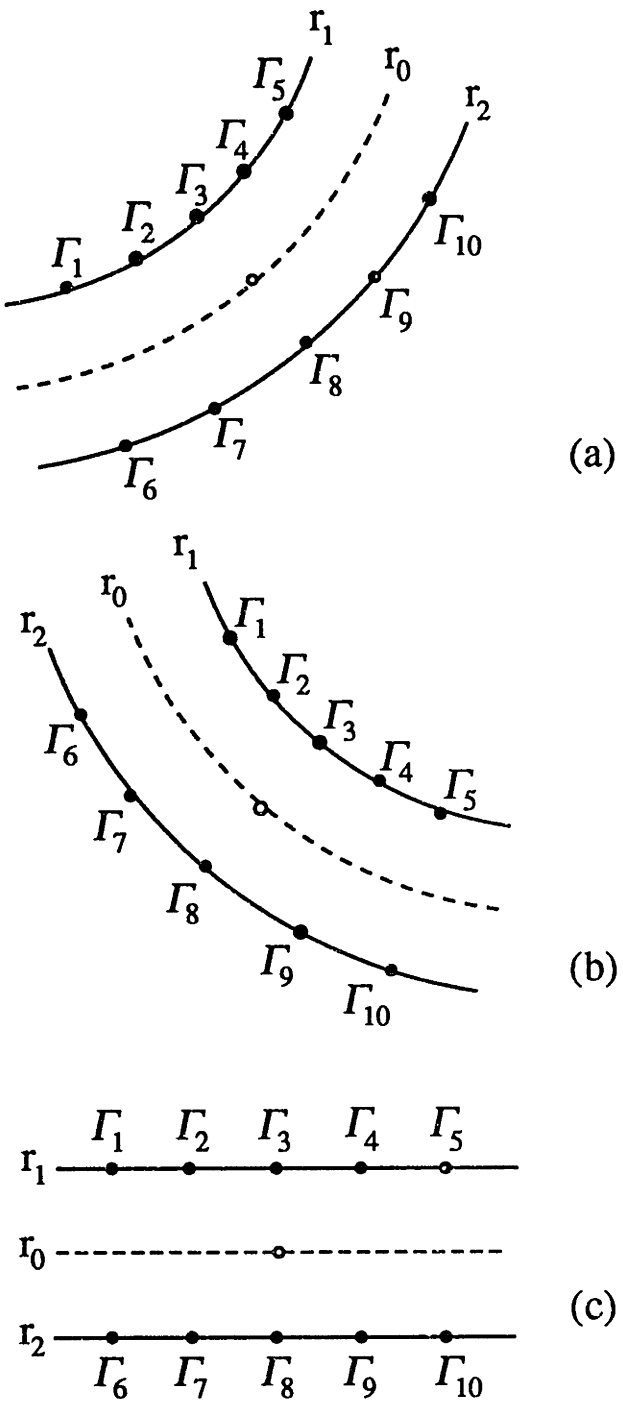

Figure 4-1: Edge Factor Analysis (a) Top Left Origin. (b) Top Right Origin (c) *LSM*

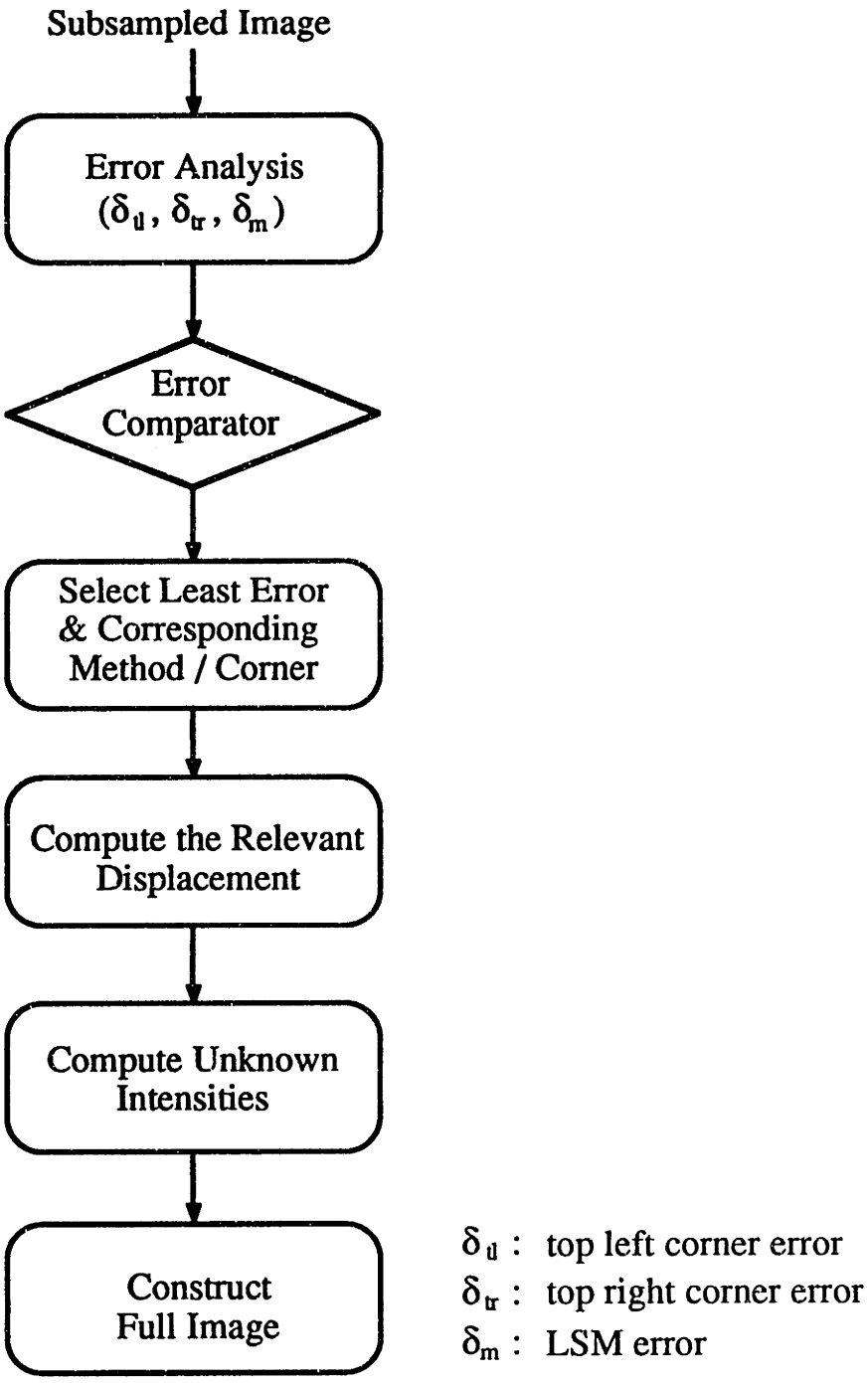

Figure 4-2: System Block Diagram

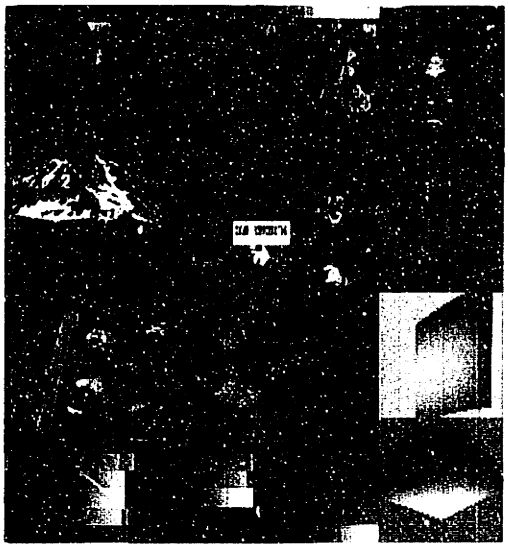

(a)

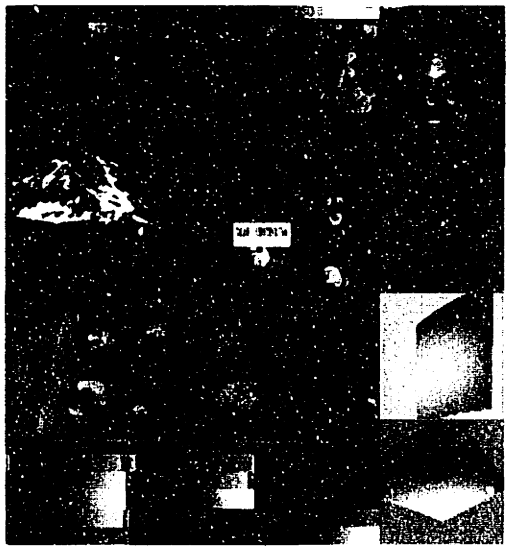

(b)

Figure (4-3):

(a) LSM-Based
(b) CCSM-Based

Chapter 5

Algorithmic Refinements and Further Research

5.1 Introduction

In this chapter, a few areas which may be of interest for future research endeavors are suggested. A set of possible refinements to the algorithm is presented, and potential extensions to a more general class of problems are discussed.

Further algorithmic refinements to the *CCSM*-based spatial interpolation method presented by this thesis, include:

- Adaptive selection of the radial distance, dR, between the "adjacent arcs" which are used in the displacement computations and luminance assignments.
- Development of a more elaborate and adaptive edge detection, and origin selection scheme.

- Development of a more accurate local neighborhood model to be used in computing the necessary image gradients.

Another area of further research which can benefit from the theory presented in this thesis is the extensibility of the *CCSM*-based approach to the more general problem of three-dimensional spatio-temporal interpolation.

5.2 Algorithmic Refinements

The algorithm presented in this thesis may be further improved by introducing additional adaptivity factors which would increase its robustness. In this section we briefly review the suggestions listed above.

5.2.1 Adjacent Arc Pair Radial Distance Selection

One feature of the proposed spatial interpolation scheme which can be an immediate target for refinement is the selection of the radial distance between the "adjacent arcs" that are used in the computation of the displacement, v_φ. Throughout the discussions, reference to this measure has been deliberately left ambiguous, since in the current implementation, the distance is manually selected from the range, $0.5 \leq dR \leq 1.3$ pel units, based on subjective considerations, and remains constant throughout the processing iterations.

Depending on the amount of local image detail, however, this fixed quantity may be too high or too low. In areas of a picture where finer details are present, for example, smaller radial distances produce better results, for selection of large values

would cause the intensities assigned to the unknown pixels to be grabbed from distant points, which may not even lie on the object to which the unknown pels belong. This will cause erroneous luminance values to be assigned to the pixels being processed, thereby causing some degradation in the reconstructed image. On the other hand, too small a radial distance in areas with low detail may not yield a sufficient dynamic range to gain optimum results. Hence, a method which utilizes some measure of local image detail is required, in order to dynamically select a proper value for the radial distance between the adjacent arcs; local variance is one such measure.

5.2.2 Edge Detection and Origin Selection

The edge detection and origin selection method used in the current implementation of the *CCSM*-based spatial interpolation algorithm, is fairly simple and crude. A more elaborate method of determining the edge factor, δ, would enhance the reconstructed images by yielding a better assessment of the local edge orientations, which would, in turn, result in a more accurate determination of the appropriate coordinate origin to be used in resolving the displacement, v_φ.

Use of directional polynomials is proposed in determining the local edge orientations. Discussion on this special class of polynomials may be found in established books on algebraic geometry. What is hoped to be gained by using directional polynomials is greater freedom and accuracy in the selection of the coordinate origin. In the current implementation, the selection is limited to one of the top image corners. This is not the optimal choice for all edge orientations. By using directional polynomials one can base the selection of the origin on the exact orientation of the local edge, in

order to adaptively determine the optimal origin at every pel processing iteration.

5.2.3 Local Neighborhood Image Model

Further improvement may be made by modeling the local image more accurately for the purpose of finding the neighborhood luminance gradients. The basis function expansion parameters used in the current implementation work reasonably well, but they are by no means intended to be normative, and more sophisticated parameters may be substituted for the ones currently installed in the system. The inherent advantage of the algorithm presented in this thesis is that it is highly modular, in that many of the components can be easily replaced with more efficient and improved ones without affecting the specification requirements imposed on the other computational modules.

5.3 Extension of the CCSM-based Algorithm to Three Dimensions

The concepts underlying the two-dimensional spatial interpolation scheme presented in this thesis may be extended to three dimensions as was Martinez's *Line Shift Model (LSM)*-based approach. This topic is discussed to some reasonable depth in the Appendix.

Appendix A

Vertico-Temporal Image Sequence Interpolation

A.1 Introduction

The concepts and notions underlying the *Concentric Circular Shift Model (CCSM)* may be easily extended to the most general class of three-dimensional problems where an image sequence undergoes resampling in all coordinate directions: horizontal, vertical, and temporal. Naturally, one can extend the notion of concentric circles to that of concentric spheres which may shift in any direction relative to each other, as long as their conincident centers remain stationary. The problem of interpolation, therefore, becomes one of computing the relative spherical shift between the neighborhood of points about the unknown pel on each of the "adjacent spherical surfaces." Once this spherical displacement has been determined, the *Constant Luminance Model (CLM)* is invoked, in order to determine the pels whose intensities correspond to that of the

unknown one.

For illustration purposes, however, we will develop the mathematics for that special case of three-dimensional problems in which resampling is performed on the vertical and temporal coordinates only. This is done for two reasons:

- The mathematical basis for the less general problem of simultaneous vertical and temporal (*i.e.,* vertico-temporal) interpolation is analogous to that of the spherical case, and no new concept is embedded in the discussion of the latter which would make its coverage more educational.

- The theory of vertico-temporal interpolation has a broader range of applications, the most well-known of which is the problem of video standards conversion between European and American systems where only temporal (*i.e.,* frame rate) and vertical (*i.e.,* line rate) resampling has to be performed.

We, therefore, apply the *CLM* by making the fundamental assumption that the luminance function remains constant along a radially parametric path in the y-t plane (*i.e.,* the vertico-temporal plane), or a plane parallel to it. In order to implement this theory, we extend the *CCSM* to include a cylindrical coordinate space representation for the luminance function, where the notion of the circularly shifting concentric circles of the two-dimensional interpolation problem is generalized to one of shifting coaxial cylinders, where the cylindrical shift has an additional degree of freedom relative to the two-dimensional model. This is depicted in Figure A-1, where the middle cylinder represents the one on which the unknown pel resides. The unknown pixel's motion is estimated, and the trajectory is reflected onto the local neighborhoods on

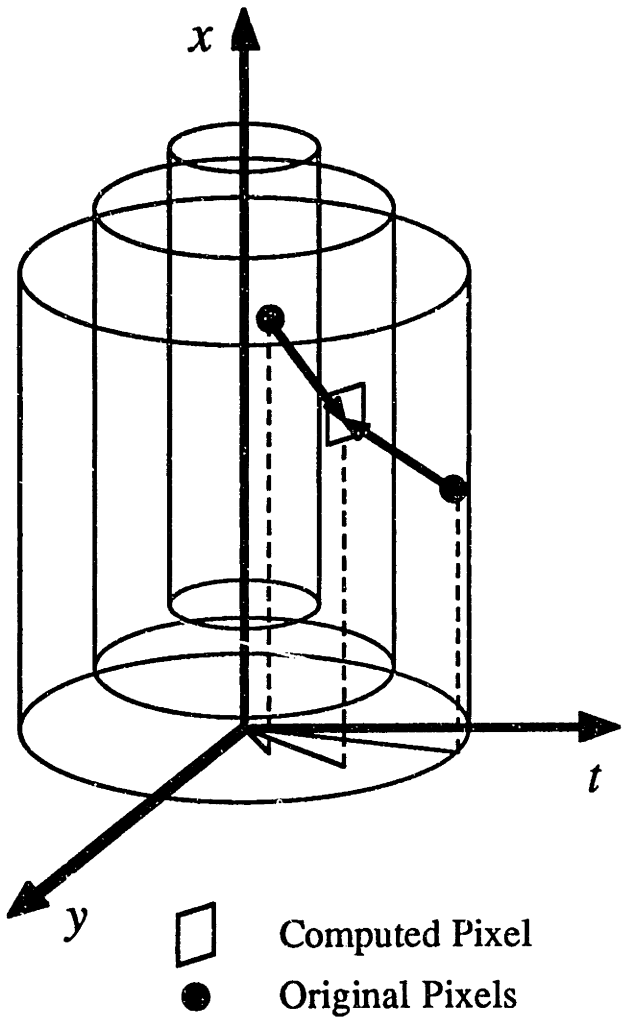

Figure A-1: Coaxial Cylindrical Shift Model

the two "adjacent cylindrical surfaces" in order to determine the unknown intensity. It is also worth noting that this Coaxial Cylindrical Shift Model is a more generalized version of the three-dimensional Cartesian extension of Martinez's *LSM*, the *Planar Shift Model (PSM)*, which is depicted in Figure A-2.

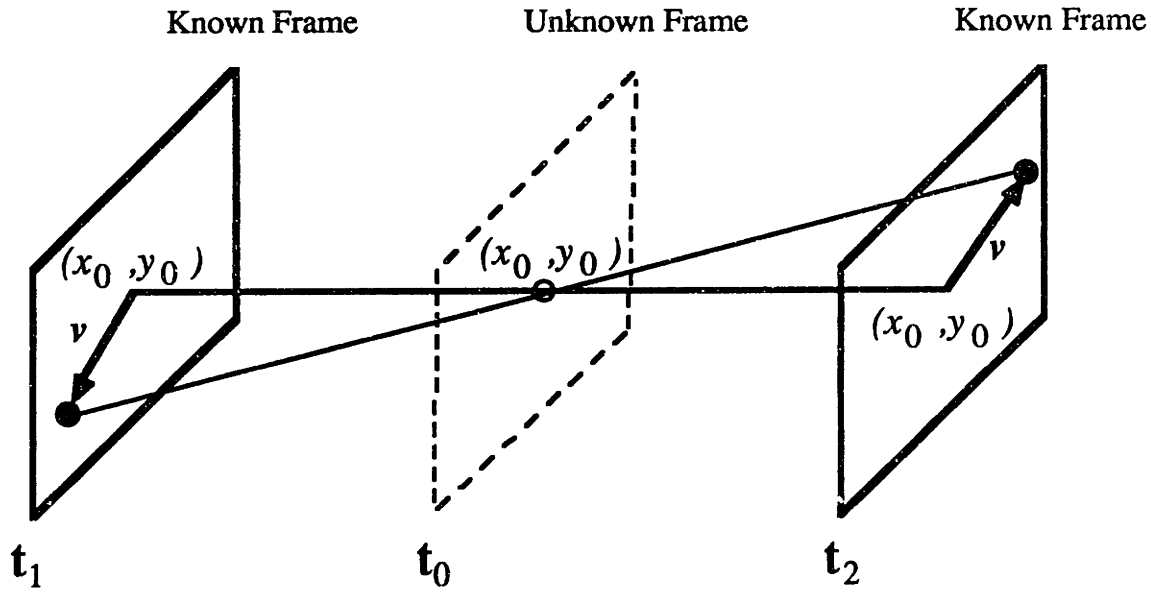

Figure A-2: Planar Shift Model

A.2 Theoretical Formulation

Our fundamental assumption requires that the "radial derivative" of the intensity be zero along the motion trajectory of the unknown pixel. This leads to the *Generalized Vertico-Temporal Constraint Equation (GVTCE)* as follows:

$$\begin{aligned} \frac{d}{dr} I\left(x(r), \theta(r), r\right) &= 0 \\ \frac{\partial I}{\partial x}\frac{dx}{dr} + \frac{\partial I}{\partial \theta}\frac{d\theta}{dr} + \frac{\partial I}{\partial r} &= 0 \\ v_r \frac{\partial I}{\partial x} + v_\theta \frac{\partial I}{\partial \theta} + \frac{\partial I}{\partial r} &= 0 \quad , \end{aligned} \tag{A.1}$$

where $v_r = \dfrac{dx}{dr}$ and $v_\theta = \dfrac{d\theta}{dr}$ are the velocity components which need to be computed in order to perform the vertico-temporal interpolation.

Note that unlike the case in the well-known spatio-temporal constraint equation, the path of differentiation along which our *GVTCE* velocity components, v_r and v_θ, are optimally computed, is not necessarily parallel to the temporal axis. Note also that our constraint equation reduces to Martinez's two-dimensional spatial interpolation equation when we set $\theta(r) = 0, \forall r$. In that case, $v_\theta = 0$ and $r = y$, and we obtain:

$$v_r = \frac{dx}{dr} = \frac{dx}{dy} = v \tag{A.2}$$

$$\frac{\partial I}{\partial r} = \frac{\partial I}{\partial y} \tag{A.3}$$

and hence,

$$v\frac{\partial I}{\partial x} + \frac{\partial I}{\partial y} = 0 \quad . \tag{A.4}$$

As was the case in the two-dimensional problem, it is impossible to find a velocity vector, $\mathbf{v} = [v_r, v_\theta]^T$, such that the *GVTCE* (A.1) is satisfied at all points within a three-dimensional region around the pel being processed. Therefore, once again we introduce an error measure, ϵ, as follows:

$$v_r\frac{\partial I}{\partial x} + v_\theta\frac{\partial I}{\partial \theta} + \frac{\partial I}{\partial r} = \epsilon \quad . \tag{A.5}$$

In order to find the velocity vector, $\mathbf{v}$, corresponding to a particular unknown pel, we assume that the required image gradients at a set of N points in the neighborhood of that position are available. We can then find the velocity vector for the desired pixel

using a least squares estimator as follows:

$$\min_{(\mathbf{v})} \left(\sum_{i=1}^{N} {\epsilon_i}^2 \right) \quad , \tag{A.6}$$

where

$$\epsilon_i = v_r \left. \frac{\partial I}{\partial x} \right|_{P_i} + v_\theta \left. \frac{\partial I}{\partial \theta} \right|_{P_i} + \left. \frac{\partial I}{\partial r} \right|_{P_i} \quad , \tag{A.7}$$

P_i represents the i^{th} point in the neighborhood. The minimization problem can then be restated as follows:

$$\min_{(v_r, v_\theta)} \left[\sum_{i=1}^{N} \left(v_r \left. \frac{\partial I}{\partial x} \right|_{P_i} + v_\theta \left. \frac{\partial I}{\partial \theta} \right|_{P_i} + \left. \frac{\partial I}{\partial r} \right|_{P_i} \right)^2 \right] \quad . \tag{A.8}$$

Since the above expression is quadratic in both v_r and v_θ, the solution can be obtained by solving a set of two linear equations in two unknowns.

Differentiating the expression, $\sum_{i=1}^{N} {\epsilon_i}^2$, with respect to v_r and v_θ, we obtain:

$$\begin{aligned} A &= \frac{\partial}{\partial v_r} \left[\sum_{i=1}^{N} \left(v_r \left. \frac{\partial I}{\partial x} \right|_{P_i} + v_\theta \left. \frac{\partial I}{\partial \theta} \right|_{P_i} + \left. \frac{\partial I}{\partial r} \right|_{P_i} \right)^2 \right] \\ &= 2 \sum_{i=1}^{N} \left[\left(v_r \left. \frac{\partial I}{\partial x} \right|_{P_i} + v_\theta \left. \frac{\partial I}{\partial \theta} \right|_{P_i} + \left. \frac{\partial I}{\partial r} \right|_{P_i} \right) \left(\left. \frac{\partial I}{\partial x} \right|_{P_i} \right) \right] \\ &= 2 \sum_{i=1}^{N} \left[v_r \left(\left. \frac{\partial I}{\partial x} \right|_{P_i} \right)^2 + v_\theta \left(\left. \frac{\partial I}{\partial x} \right|_{P_i} \right) \left(\left. \frac{\partial I}{\partial \theta} \right|_{P_i} \right) + \left(\left. \frac{\partial I}{\partial x} \right|_{P_i} \right) \left(\left. \frac{\partial I}{\partial r} \right|_{P_i} \right) \right] \end{aligned} \tag{A.9}$$

$$\begin{aligned} B &= \frac{\partial}{\partial v_\theta} \left[\sum_{i=1}^{N} \left(v_r \left. \frac{\partial I}{\partial x} \right|_{P_i} + v_\theta \left. \frac{\partial I}{\partial \theta} \right|_{P_i} + \left. \frac{\partial I}{\partial r} \right|_{P_i} \right)^2 \right] \\ &= 2 \sum_{i=1}^{N} \left[\left(v_r \left. \frac{\partial I}{\partial x} \right|_{P_i} + v_\theta \left. \frac{\partial I}{\partial \theta} \right|_{P_i} + \left. \frac{\partial I}{\partial r} \right|_{P_i} \right) \left(\left. \frac{\partial I}{\partial \theta} \right|_{P_i} \right) \right] \\ &= 2 \sum_{i=1}^{N} \left[v_r \left(\left. \frac{\partial I}{\partial x} \right|_{P_i} \right) \left(\left. \frac{\partial I}{\partial \theta} \right|_{P_i} \right) + v_\theta \left(\left. \frac{\partial I}{\partial \theta} \right|_{P_i} \right)^2 + \left(\left. \frac{\partial I}{\partial \theta} \right|_{P_i} \right) \left(\left. \frac{\partial I}{\partial r} \right|_{P_i} \right) \right] \quad . \end{aligned} \tag{A.10}$$

To find the optimal solution, we allow $A = 0$ and $B = 0$. This is equivalent to the following set of equations:

$$\begin{cases} \left[\sum_{i=1}^{N}\left(\left.\frac{\partial I}{\partial x}\right|_{P_i}\right)^2\right] v_r + \left[\sum_{i=1}^{N}\left(\left.\frac{\partial I}{\partial x}\right|_{P_i}\right)\left(\left.\frac{\partial I}{\partial \theta}\right|_{P_i}\right)\right] v_\theta + \sum_{i=1}^{N}\left(\left.\frac{\partial I}{\partial x}\right|_{P_i}\right)\left(\left.\frac{\partial I}{\partial r}\right|_{P_i}\right) = 0 \\ \left[\sum_{i=1}^{N}\left(\left.\frac{\partial I}{\partial x}\right|_{P_i}\right)\left(\left.\frac{\partial I}{\partial \theta}\right|_{P_i}\right)\right] v_r + \left[\sum_{i=1}^{N}\left(\left.\frac{\partial I}{\partial \theta}\right|_{P_i}\right)^2\right] v_\theta + \sum_{i=1}^{N}\left(\left.\frac{\partial I}{\partial \theta}\right|_{P_i}\right)\left(\left.\frac{\partial I}{\partial r}\right|_{P_i}\right) = 0 \end{cases} \tag{A.11}$$

which we can, in turn, rewrite in matrix form as follows:

$$\begin{pmatrix} \sum_{i=1}^{N}\left(\left.\frac{\partial I}{\partial x}\right|_{P_i}\right)^2 & \sum_{i=1}^{N}\left(\left.\frac{\partial I}{\partial x}\right|_{P_i}\right)\left(\left.\frac{\partial I}{\partial \theta}\right|_{P_i}\right) \\ \sum_{i=1}^{N}\left(\left.\frac{\partial I}{\partial x}\right|_{P_i}\right)\left(\left.\frac{\partial I}{\partial \theta}\right|_{P_i}\right) & \sum_{i=1}^{N}\left(\left.\frac{\partial I}{\partial \theta}\right|_{P_i}\right)^2 \end{pmatrix} \begin{pmatrix} v_r \\ v_\theta \end{pmatrix} = - \begin{pmatrix} \sum_{i=1}^{N}\left(\left.\frac{\partial I}{\partial x}\right|_{P_i}\right)\left(\left.\frac{\partial I}{\partial r}\right|_{P_i}\right) \\ \sum_{i=1}^{N}\left(\left.\frac{\partial I}{\partial \theta}\right|_{P_i}\right)\left(\left.\frac{\partial I}{\partial r}\right|_{P_i}\right) \end{pmatrix} . \tag{A.12}$$

Solving Equation (A.12) yields the desired least squares optimal values for the two velocity components, v_r and v_θ.

A.3 Computation of the Partial Derivatives

A problem which needs to be addressed at this point is the computation of the actual luminance partial derivatives $\frac{\partial I}{\partial x}$, $\frac{\partial I}{\partial \theta}$, and $\frac{\partial I}{\partial r}$, so that the velocity components, v_r and v_θ, may be computed from the matrix Equation (A.12). In order to compute these

gradients, we model the luminance function in cylindrical coordinates. Once again, as we did in the two-dimensional spatial interpolation problem, we use a parametric polynomial expansion method to model the local image. It should be noted, however, that this model only serves to facilitate computation of the motion parameters, v_r and v_θ, and should not be used in calculation of the desired intensities which require subpixel accuracy.

We propose the following model for the luminance function:

$$\hat{I}(x,\theta,r) = \sum_{j=1}^{P} f_j \Phi_j(x,\theta,r) \ , \tag{A.13}$$

where the f_j's are the luminance function model parameters which we have to estimate, and the $\Phi_j(x,\theta,r)$'s form a set of P basis functions used to span the image function space. A possible set of such basis functions is given below:

$$\begin{array}{lll} \Phi_1(x,\theta,r) = 1 & \Phi_2(x,\theta,r) = x & \Phi_3(x,\theta,r) = \theta \\ \Phi_4(x,\theta,r) = r & \Phi_5(x,\theta,r) = x^2 & \Phi_6(x,\theta,r) = \theta^2 \\ \Phi_7(x,\theta,r) = x\,\theta & \Phi_8(x,\theta,r) = x\,r & \Phi_9(x,\theta,r) = r\,\theta \end{array} \ . \tag{A.14}$$

With Equation (A.12) specified, and the local image gradients computed, the task of solving for the unknown velocity components, v_r and v_θ, becomes as straightforward as that of the two-dimensional interpolation algorithm.

Bibliography

[1] "Encoding parameters of digital television for studios." CCIR Recommendation 601-1 XVIth Plenary Assembly Dubrovnik, 1986. Vol XI, Part 1, pp 319 – 328.

[2] H. S. Hou and H. C. Andrews, "Cubic splines for image interpolation and digital filtering," *IEEE Trans. Acoustics, Speech, and Signal Processing*, vol. 26, pp. 508 – 517, December 1978.

[3] D. M. Martinez and J. S. Lim, "Spatial interpolation of interlaced television pictures," in *Proceedings of ICASSP*, 1989.

[4] M. Isnardi, *Modeling the Television Process.* PhD thesis, Massachusetts Institute of Technology, May 1986.

[5] D. M. Martinez, *Model-Based Motion Estimation and its Application to Restoration and Interpolation of Motion Pictures.* PhD thesis, Massachusetts Institute of Technology, August 1986.

[6] G. Arfken, *Mathematical Methods for Physicists, 3rd Ed.* Academic Press, 1985.

[7] A. V. Oppenheim and R. W. Schafer, *Discrete-Time Signal Processing.* Prentice-Hall, 1989.

[8] J. S. Lim, *Two-Dimensional Signal and Image Processing.* Prentice Hall, 1990.

[9] R. E. Crochiere and L. R. Rabiner, *Multirate Digital Signal Processing.* Prentice Hall, 1983.

[10] A. V. Oppenheim, A. S. Willsky, and I. T. Young, *Signals and Systems.* Prentice Hall, 1983.

[11] B. Ayazifar and J. S. Lim, "Pel-adaptive model-based interpolation of spatially subsampled images," in *Proceedings of ICASSP*, 1992.

[12] K. H. Barratt and J. H. Taylor, "Line interpolation," *IBA Tech. Rev.*, vol. 8, September 1976. Digital Video Processing – DICE.

[13] R. W. Schafer and L. R. Rabiner, "A digital signal processing approach to interpolation," *Proceedings of IEEE*, vol. 61, June 1973.

[14] R. N. Hurst and K. H. Powers, "The development of international television standards," *RCA Engineer*, vol. 28, September/October 1983.

[15] C. K. P. Clarke, "Future television systems: Comparison of sequential and interlaced scanning," tech. rep., Research Department, Engineering Division, The British Broadcasting Corporation, November 1987.

[16] W. F. Schreiber, *Fundamentals of Electronic Imaging Systems.* Springer-Verlag, 1986.

[17] G. Strang, *Introduction to Applied Mathematics.* Wellesley – Cambridge Press, 1986.

[18] D. E. Dudgeon and R. M. Mersereau, *Multidimensional Digital Signal Processing.* Prentice Hall, 1984.

[19] A. N. Netravali and B. G. Haskell, *Digital Pictures: Representation and Compression.* Plenum Press, 1988.

[20] C. Cafforio and F. Rocca, "Methods for measuring small displacements of television images," *IEEE Transactions on Information Theory*, vol. IT-22, pp. 573 – 579, September 1976.

[21] C. K. P. Clarke and N. E. Tanton, "Digital standards conversion: Interpolation theory and aperture synthesis," Tech. Rep. UDC 621.397.65, British Broadcasting Corporation, December 1984.

[22] B. K. P. Horn and B. G. Schunck, "Determining optical flow," *Artificial Intelligence*, no. 17, pp. 185 – 203, 1981.

[23] R. Paquin and E. Dubois, "A spatio-temporal gradient method for estimating the displacement field in time-varying imagery," *Computer Vision, Graphics, and Image Processing*, no. 21, pp. 205 – 221, 1983.

[24] J. W. Roach and J. K. Aggarwal, "Determining the movement of objects from a sequence of images," *IEEE Transactions on Pattern Analysis and Machine Intelligence*, vol. PAMI-2, pp. 554 – 203, November 1980.